Research Square

Preprints are preliminary reports that have not undergone peer review.
They should not be considered conclusive, used to inform clinical practice,
or referenced by the media as validated information.

Identification and Neuroprotective Evaluation of Phytoconstituents from Ailanthus excelsa: In Silico Docking and In Vitro Acetylcholinesterase Inhibition Assay

Vijayabaskaran Manickam

vijayabass@gmail.co

J. K. K. Nattraja college of Pharmacy, Affiliated to The Tamil Nadu Dr. MGR Medical University

Manikandan Karuppaiya

J. K. K. Nattraja college of Pharmacy, Affiliated to The Tamil Nadu Dr. MGR Medical University

Madeswaran Arumugam

Professor & Head, Karpagam College of Pharmacy, Affiliated to The Tamil Nadu Dr. MGR Medical University

Research Article

Keywords: Phytoconstituents, FTIR analysis, 4-Hydroxycoumarin, Ferulic acid

Posted Date: November 3rd, 2026

DOI: https://doi.org/10.21203/rs.3.rs-11407874/v1

License: This work is licensed under a Creative Commons Attribution 4.0 International License.
Read Full License

Additional Declarations: No competing interests reported.

Abstract

The plant *Ailanthus excelsa* exhibits considerable antioxidant, cytotoxic, and anti-inflammatory effects. The present study aimed to characterize the bioactive phytoconstituents of *A. excelsa* and evaluate their neuroprotective potential through *in silico* modeling and *in vitro* acetylcholinesterase (AChE) inhibition assay. Based on the peaks obtained from Fourier-transform infrared spectroscopy (FTIR) analysis, thirteen distinct functional groups corresponding to potential phytoconstituents were identified in *A. excelsa*. The identified phytoconstituents obeyed Lipinski's Rule of Five and were further evaluated via *in silico* docking studies against the acetylcholinesterase target enzyme using AutoDock 4.2 software. Rivastigmine, a standard cholinesterase inhibitor, was used to compare the enzyme inhibitory potentials of the selected compounds. The computational *in silico* investigation revealed that the compounds possessed excellent docking scores and favorable binding orientations with the acetylcholinesterase enzyme, outperforming the standard drug. A uniform decrease in binding energy was observed for all phytoconstituents against the target enzyme, with values ranging from − 8.36 kcal/mol to -3.82 kcal/mol. Specifically, docking results demonstrated that 4-hydroxycoumarin and ferulic acid possessed notable anti-cholinesterase activity compared to the other phytoconstituents and rivastigmine. In the *in vitro* enzyme inhibition assay, the half-maximal inhibitory concentration IC_{50} of ferulic acid was found to be 7.5468 ± 1.42 µg/ml, while 4-hydroxycoumarin exhibited an IC_{50} of 3.4562 ± 0.84 µg/ml, compared to 3.913 ± 0.48 µg/ml for the standard rivastigmine. In conclusion, 4-hydroxycoumarin and ferulic acid possess a potential role in neuroprotection and could be developed as promising drug candidates against neurodegenerative diseases.

INTRODUCTION

The phrase "*in silico*" pertains to computer-driven experimentation and is a contemporary term linked to the better-known biological concepts "*in vivo*" and "*in vitro*" (Natesh et al., 2023). Computational or *in silico* techniques are assisting us in decision-making and virtually simulating every aspect of drug discovery and development, bringing the pharmaceutical sector nearer to engineering-oriented fields (Crampon et al., 2022). The purpose of computational models is to improve prediction based on already known information. It is thought that computational methods can improve industry efficiency and are becoming a greater and more important part of drug research and development. They are anticipated to drastically reduce traditional resource requirements by limiting and concentrating chemical synthesis and biological testing (Wadood et al., 2013).

Molecular docking algorithms provide a scoring function to rank the docked ligands based on the binding energy of the protein-ligand complexes, and they also make quantitative predictions regarding the strength of the association or binding. These processes are performed in a cycle where the conformation of the ligand is assessed using specific scoring functions (Das et al., 2022). Molecular docking is commonly used in modern drug design to study how drugs interact with their target proteins and to predict the orientation of potential drug candidates. This helps estimate the binding affinity and activity of small molecules, making it an essential tool in drug discovery (Babitha et al., 2015).

Global changes in population trends are likely to make neurodegenerative diseases (NDs) a major challenge for public health and medical care in the future. These diseases are primarily linked to serious mental health issues, characterized by the loss or damage of neurons. This loss of neurons results in various psychological and psychiatric problems, as well as long-term physical disabilities (Aaron et al., 2017).

Alzheimer's disease begins with the loss of short-term memory, particularly affecting the ability to recall recent events, and eventually leads to a person losing their sense of identity. Approximately 50% of adults who are 85 years old or older are affected by Alzheimer's disease, which is the primary cause of between 50% and 70% of all dementia cases. As people are living longer, this condition presents a major challenge to society and has a significant impact on the health and well-being of older adults and their families. The two primary brain changes associated with Alzheimer's are neurofibrillary tangles and senile plaques. Neurofibrillary tangles are made up of amyloid β (Aβ) peptides, whereas senile plaques consist of hyperphosphorylated Tau protein (Ajit et al., 2018).

A flavoprotein is characterized as homodimeric, with a glutaredoxin (Grx) domain connected to a standard thioredoxin reductase (TR) domain in each of its subunits. In Schistosoma, the maintenance of redox homeostasis is entirely dependent on TGR, which facilitates the transfer of nicotinamide adenine dinucleotide phosphate to reduce equivalents for thioredoxin and glutathione. TGR is the sole enzyme capable of reducing both thioredoxin and glutathione disulfide, indicating that the parasite's redox mechanism is significantly dependent on this enzyme (Rashed et al., 2013). The aim of the current study is to characterize the bioactive phytoconstituents of *A. excelsa* and evaluate their neuroprotective potential through *in silico* modeling and *in vitro* acetylcholinesterase (AChE) inhibition assay.

MATERIALS AND METHODS

Software utilized:

Molinspiration software, AutoDock 4.2, ChemSketch, RCSB protein data bank, Accerly's Discovery Studio Viewer 4.0.1, and Online SMILES translator.

Chemicals Used:

Sigma Aldrich, USA was the supplier of hydroxy benzoyl chloride, dihydroxy acetophenone, methyl benzoyl chloride, and anhydrous potassium carbonate. The study's other medications and substances were all of analytical quality and purchased commercially. The Kohfler melting point equipment was used to determine the melting points. The Jasco V-530 UV-VIS spectrophotometer was used to record UV spectra. Using KBr disks on a Perkin Elmer FT/IR spectrophotometer 1650, the infrared spectra were acquired.

Preparation of Ailanthus excelsa Extract

Preparation of Ailanthus excelsa Extract
Leaves of *Ailanthus excelsa* were collected, authenticated by The Tamil Nadu Agricultural University [BSI/SRC/23/2024-25/Tech./572] and shade-dried. The dried leaves were pulverized into a fine powder. Ethanolic Soxhlet extraction was performed using 100 g of dry powder and 250 mL of ethanol. The extract was evaporated under reduced pressure, and the crude extract was defatted with petroleum ether. The defatted extract was dried and partitioned between water and n-butanol. The resultant n-butanol fraction was used for the study and further analysis (Vargas-Madriz et al., 2020).

Characterization of the Phytoconstituents Using Fourier-Transform Infrared Spectroscopy

FTIR has demonstrated its effectiveness as a crucial instrument for characterizing and identifying compounds or functional groups (chemical bonds) found in an unknown plant extract mixture. Moreover, the FTIR spectra of pure compounds are typically so distinctive that they serve as a molecular "fingerprint".

For many common plant compounds, the spectrum of an unknown substance can be recognized by comparing it to a database of known compounds. FTIR sample preparation can be accomplished in various ways. For liquid samples, the simplest method involves placing a drop of the sample between two sodium chloride plates. This drop creates a thin film between the plates. Solid samples can be ground with potassium bromide (KBr) and then pressed into a thin pellet for analysis. Alternatively, solid samples may be dissolved in a solvent like methylene chloride, and the resulting solution is applied to a single salt plate. The solvent is subsequently evaporated, leaving a thin film of the original substance on the plate (Sasidharan et al., 2011).

In the present study, the following samples were used dry powder of *Ailanthus excelsa* leaves and n-butanol extract of *Ailanthus excelsa*. The FTIR was used to characterize and identify the phytoconstituents present in the *Ailanthus excelsa*.

Evaluation of Drug Likeness Properties

During drug development, pharmacokinetic studies and optimization benefit from the use of drug similarity principles. Currently, molecular description techniques like the "Rule-of-Five" are used to categorize and forecast medication solubility, chemical stability, and bioavailability. By analyzing biologically significant factors, the assessment aims to determine how similar a molecule is to a medicine (Bang et al., 2025).

The drug-likeness score and the computation of steric, hydrophobic, electronic, and hydrogen bonding properties were used to characterize pharmacologically active substituents. The Lipinski's Rule-of-Five is

one example of a molecular descriptor that was developed as logically informative and predictive. By gathering data on solubility, diffusion, Log P, molecular weight, and other factors, the improved oral absorption of the ligands and drug similarity scores were created. The Lipinski's rule of five was assessed using Molinspiration software (Karami et al., 2022).

In silico docking study on acetylcholinesterase enzyme using Autodock 4.2

Enzyme identification for in silico docking

The acetylcholinesterase enzyme's crystal structure (PDB ID: 1GQR) was acquired from the protein data library of the Research Collaborative for Structural Bioinformatics (Fig. 1). Additional *in silico* research was conducted using the improved protein (Vijayabaskaran et al., 2025; Madeswaran et al., 2023).

The interaction between proteins and ligands was demonstrated. Holding down the right key while pressing Ctrl will zoom it in and boost the contrast. The atomic resemblance potentials for each atom in the chosen ligands were pre-calculated in order to achieve rapid energy evaluation. The AutoGrid procedure involved enclosing the target on a three-dimensional grid point and determining the energy of contact for every atom in the ligand. A population size of 150 individuals, a maximum of 27000 generations, the number of top individuals that automatically survive to the next generation of 1, 2.5 million energy evaluations, a crossover rate of 0.8, a mutation rate of 0.02, 10 docking runs, and random initial positions and conformations were the docking factors selected for the Lamarckian genetic algorithm. The likelihood of conducting a local search on the population's single compound was set at 0.06. The expected binding energy was computed using AutoDock, which was run multiple times to produce different docked conformations (Madeswaran and Mohan, 2023; Tokali et al., 2023).
Characterization of Selected Phytoconstituents:
IR and mass spectroscopy were used to determine the structures of the produced molecules (Prafulla et al., 2021). Shimadzu 8000 or Perkin-Elmer series 1600 spectrometers were used to record infrared (IR) spectra of solid materials using KBr pellets as thin films. The mass-to-charge ratio (m/z) of the molecules in the active phytoconstituents sample was measured in order to identify and quantify them using mass spectral data (Tang et al., 2004).

In vitro Acetylcholinesterase Inhibition

The test to measure enzyme inhibition was done using the Ellman method, as described by Ellman *et al.*, in 1961. About 1.3 ml of the TrisHCl buffer, which had a pH of 8.0 and was 50 mM, was mixed with 0.4 ml of the drug solution at different concentrations. Then, 0.1 ml of AChE, which was at a concentration of 0.28 U per ml, was added to this mixture. This mixture was left to sit for 15 minutes.Then, 0.3 ml of Acetylthiocholine iodide, which was prepared at a concentration of 0.023 mg per ml, and 1.9 ml of DTNB solution, which was at a concentration of 3 mM, were added to it. After the final reaction mixture was prepared, it was left at room temperature for 30 minutes to continue reacting.Then, the amount of light

absorbed by the reaction mixture was measured at a wavelength of 405 nm. The test was performed three times, and the results were shown as the average plus or minus the standard error of the mean. The percentage inhibition was determined for the chosen flavonoids (Sacan and Yanardag, 2010).

Statistical analysis:

One-way ANOVA was used for statistical analysis, followed by Dunnett's test. The results are shown as the mean ± SEM from each group. P-values below 0.05 were considered significant (Shin et al., 2018).

RESULTS

Fourier-transform infrared spectroscopy (FTIR)

The FTIR results have shown that the functional group of Dry powder and the n-butanol Extract were almost similar. Hence the Phytoconstituents were actively present.

The FTIR (Fourier Transform Infrared) spectrum of an n-butanol extract of *Ailanthus excelsa* acts as a molecular fingerprint, identifying the specific functional groups of bioactive secondary metabolites concentrated by this solvent (Fig. 2). When compared to a standard (often a high-purity reference extract or a standard pharmacological drug), these peaks confirmed the presence and concentration of therapeutic compounds like Selinidin, Trans piceattannol, P-hydroxyphenethyl anisate, 4-o-feruloylquinic acid, p-coumaroylquinic acid, 4-hydroxy coumarin, Ferulic acid, Salicylic acid, 5-hydroxy ferulic acid, Caffeic acid, Malic acid, p-coumaroyl hexose, Quinic acid (Table 1).

Table 1
FTIR Interpretation of the functional group analysis

S.NO	Standard Range (cm^{-1})	Observed Peak (cm^{-1})	Functional Group
1.	**3200–3600**	**3540–3280**	**O–H (alcohol / phenol)**
2.	2850–3000	2997–2850	C–H (alkanes)
3.	1900–2000	~ 1978	Aromatic overtones
4.	1600–1680	1660–1600	C = C (alkene / aromatic) or C = O (conjugated)
5.	1450–1500	1465–1440	C–H (alkanes)
6.	1370–1390	1380–1375	C–H (methyl)
7.	1200–1350	1320–1250	C–N (amines) or C–O (phenols)
8.	1150–1250	1215–1150	C–O (alcohols, esters)
9.	1000–1150	1125–1025	C–O / C–O–C
10.	800–1000	950–850	=C–H (alkenes, aromatics)
11.	3200–3600	3540–3280	O–H (alcohol / phenol)

The n-butanol fraction is typically a polyphenolic-rich extract. Its spectral profile usually displays these characteristic bands. The functional groups identified by these peaks correlate with the plant's medicinal profile. Hence, based on the peaks obtained by the FTIR analysis it was confirmed that the possible functional groups may present in the *Ailanthus excelsa*.

Based on the review of literature the *Ailanthus excels* possess the following active phytoconstituents such as, Selinidin, Trans piceattannol, P-hydroxyphenethyl anisate, 4-o-feruloylquinic acid, p-coumaroylquinic acid, 4-hydroxy coumarin, Ferulic acid, Salicylic acid, 5-hydroxy ferulic acid, Caffeic acid, Malic acid, p-coumaroyl hexose, Quinic acid. The compounds functional groups were confirmed with the FTIR analysis. These compounds were further taken for the consideration of *in silico* and *in vitro* evaluation against acetylcholinesterase target for the management of neurodegenerative diseases.

To promote the discovery and development of new pharmaceuticals, significant efforts are underway to assess the similar 'drug-like' characteristics of molecules during the initial phases of the discovery-research process. Various strategies exist to address this challenge, but the most straightforward and widely adopted method was formulated by Chris Lipinski and his team at Pfizer, commonly known as the Lipinski Rules or the Rule of Five (ROF). The Rule of Five (ROF) serves as a guideline for assessing drug likeness or determining whether a chemical compound with specific pharmacological or biological activity possesses attributes that would render it a likely orally active drug in humans.

Table 2
Druggability of the selected phytoconstituents

S.No	Compounds	Molecular weight	Log p value	nON *	*nOHNH* **	Rotatable Bonds	No. of violations
1.	**Selinidin**	**328.36**	**4.12**	**5**	**0**	**3**	**0**
2.	Trans piceattannol	244.25	2.50	4	4	2	0
3.	P-hydroxyphenethyl anisate	272.30	3.49	4	1	6	0
4.	4-o-feruloylquinic acid	354.31	-0.45	9	6	5	1
5.	P-coumaroylquinic acid	338.31	-0.18	8	5	5	0
6.	4-hydroxy coumarin	150.18	1.55	2	2	2	0
7.	Ferulic acid	194.19	1.25	4	2	3	0
8.	Salicylic acid	138.12	1.87	3	2	1	0
9.	5-hydroxy ferulic acid	210.19	0.96	5	3	3	0
10.	Caffeic acid	312.23	-0.61	9	5	7	0
11.	Malic acid	134.09	-1.57	5	3	3	0
12.	P-coumaroyl hexose	655.15	10.28	2	0	22	2
13.	Quinic acid	192.17	-2.33	6	5	1	0
* Number of hydrogen bond acceptors							
** *Number of hydrogen bonds donors*							

Acknowledging the significance of retrospective analyses of drug candidates, as initially established and formalized by Lipinski, various researchers have identified different combinations of criteria that serve as crucial predictors of permeability. An additional guideline was introduced by Veber, who assessed the oral bioavailability of compounds and compared their permeability with molecular flexibility, which can be quantified by the number of rotatable bonds. Estimating the number of rotatable bonds facilitates the correlation of permeability characteristics without factoring in molecular weight. It has been determined that compounds possessing more than ten rotatable bonds typically exhibit poor permeability. Furthermore, Veber concluded that a high polar surface area contributes to reduced permeability (Table 2).

Computed properties such as molecular weight, molecular branching, hydrogen bonding, aromatic density, and logP were analyzed and compared against lists of drugs with available CNS activity data. The molecular weight, degree of branching, number of rotatable bonds, and number of hydrogen bonds exhibited the strongest correlation with CNS permeability, indicating that increases in these values lead to decreased CNS exposure. Likewise, an increase in aromatic density, the number of H-bond donors, or cLogP values predicted compounds with enhanced CNS permeability.

In molecular docking, a negative score signifies a favorable interaction, with more negative values indicating stronger binding. Therefore, the lowest (most negative) binding score suggests the highest likelihood of a stable and strong interaction between the protein and the ligand. The smaller the KD value, the greater the binding affinity of the ligand for its target. The larger the KD value, the more weakly the target molecule and ligand are attracted to and bind to one another.

The goals of molecular docking are the identification of a ligand that binds to a specific receptor binding site and the identification of its preferred, energetically most favorable, binding pose. In order to accomplish this task, molecular docking tools will generate a set of different ligand binding poses and use a scoring function to estimate binding affinities for the generated ligand poses in order to determine the best binding mode.

Table 3
Binding energies of phytoconstituents against acetylcholinesterase target enzyme

S.No	Compounds	Binding energies (Kcal/mol)				
1.	**Selinidin**	**-5.75**	**-5.46**	**-5.27**	**-5.14**	**-4.92**
2.	Trans piceatannol	-4.80	-4.73	-4.43	-4.38	-4.16
3.	P-hydroxyphenethyl anisate	-6.38	-6.20	-5.81	-5.35	-5.08
4.	4-o-feruloylquinic acid	-5.36	-4.86	-4.61	-4.42	-4.12
5.	P-coumaroylquinic acid	-5.48	-5.26	-5.34	-5.17	-4.84
6.	4-hydroxy coumarin	-8.36	-8.21	-8.08	-7.82	-7.48
7.	Ferulic acid	-8.08	-7.95	-7.84	-7.3	-6.25
8.	Salicylic acid	-3.82	-3.76	-3.54	-3.48	-3.24
9.	5-hydroxy ferulic acid	-4.53	-3.75	-3.35	-3.26	-2.48
10.	Caffeic acid	-4.84	-4.13	-4.56	-4.4	-4.16
11.	Malic acid	-4.45	-3.7	-3.63	-3.54	-3.43
12.	P-coumaroyl hexose	-4.74	-3.88	-3.79	-3.61	-3.54
13.	Quinic acid	-4.81	-4.49	-4.48	-3.67	-4.25
14.	Rivastigmine	-5.21	-5.11	-3.65	-3.65	-3.24

We found a decrease in binding energy of all the phytoconstituents against acetylcholinesterase target enzyme. The phytoconstituents showed binding energy ranging between − 8.36 kcal/mol to -3.82 kcal/mol (Table 3). 4-hydroxy coumarin had excellent binding energy (-8.36 kcal/mol) when compared to the standard (-5.21 kcal/mol). This result further proved that 4-hydroxy coumarin and Ferulic acid consist of notable anti-cholinesterase activity compared to the all other phytoconstituents and standard rivastigmine.

Table 4
Inhibition constant of phytoconstituents against acetylcholinesterase target enzyme

S.No	Compounds	Inhibition Constant (mM / µM*)				
1.	**Selinidin**	**289.27***	**361.06***	**479.0***	**1.17**	**1.24**
2.	Trans piceatannol	47.61*	64.15*	78.03*	137.36*	264.71*
3.	P-hydroxyphenethyl anisate	3.93	4.36	23.72	31.19	33.82
4.	4-o-feruloylquinic acid	542.32*	755.63*	851.41*	1.23	1.32
5.	P-coumaroyl quinic acid	92.44*	129.57*	172.6*	344.73*	434.38*
6.	4-hydroxy coumarin	4.67*	14.22*	16.28*	19.26*	21.18*
7.	Ferulic acid	5.46*	9.79	21.84	25.48	77.29
8.	Salicylic acid	44.91	32.92	19.29	196.23*	218.7*
9.	5-hydroxy ferulic acid	45.48*	154.61*	725.5*	810.64*	984.86*
10.	Caffeic acid	194.83*	268.7*	212.69*	282.43*	226.74*
11.	Malic acid	14.91	22.92	49.29	73.74	75.03
12.	P-coumaroyl hexose	12.4*	12.43*	12.83*	22.9*	18.14*
13.	Quinic acid	49.18*	72.46*	91.35*	1.21	1.27
14.	Rivastigmine	22.61*	36.15*	48.03*	69.36*	84.71*

The inhibition constant (Ki) is a key parameter used to describe the binding affinity between an inhibitor and its target enzyme or receptor. It represents the equilibrium dissociation constant for the inhibitor–enzyme complex and reflects the concentration of inhibitor required to occupy half of the available binding sites at equilibrium. Because Ki is directly related to binding strength, it is widely used to compare the potency of different inhibitors. A lower Ki value indicates higher binding affinity and therefore a more potent inhibitor, while a higher Ki suggests weaker binding.

Experimentally, Ki is determined through enzyme kinetic assays based on different inhibition mechanisms, such as competitive, non competitive, or uncompetitive inhibition. In computational drug design, Ki can be estimated from predicted binding free energy (ΔG) values obtained from molecular docking studies. These computational estimates assist in ranking ligand candidates and guiding the

design of more effective inhibitors. Thus, Ki plays a crucial role in biochemistry and structure-based drug discovery, offering valuable insight into inhibitor efficiency, selectivity, and therapeutic potential.

In the present study, found a decrease in inhibition constant of all the phytoconstituents against acetylcholinesterase target enzyme similar to that of binding energy. The phytoconstituents showed inhibition constant ranging between 4.67 µM to 44.91 mM (Table 4). 4-hydroxy coumarin had excellent binding energy 4.67 µM when compared to the standard 22.62 µM. This result further proved that 4-hydroxy coumarin and Ferulic acid consist of notable cholinesterase inhibition constant values compared to the all other phytoconstituents and standard rivastigmine.

Table 5
Intermolecular energy of phytoconstituents against acetylcholinesterase target enzyme

S. No	Compounds	Intermolecular Energies (Kcal/mol)				
1.	**Selinidin**	**-7.38**	**-7.21**	**-6.68**	**-6.65**	**-6.41**
2.	Trans piceatannol	-7.51	-7.39	-7.06	-6.67	-6.5
3.	P-hydroxyphenethyl anisate	-7.40	-6.39	-6.23	-6.18	-5.75
4.	4-o-feruloylquinic acid	-5.15	-5.08	-4.87	-4.82	-4.91
5.	P-coumaroylquinic acid	-6.79	-6.61	-6.22	-6.08	-6.01
6.	4-hydroxy coumarin	-8.17	-8.4	-8.32	-8.22	-7.76
7.	Ferulic acid	-8.03	-8.57	-8.33	-8.32	-8.16
8.	Salicylic acid	-5.54	-5.31	-4.71	-4.29	-3.69
9.	5-hydroxy ferulic acid	-6.99	-6.07	-6.01	-5.89	-5.68
10.	Caffeic acid	-7.38	-7.21	-6.68	-6.65	-6.41
11.	Malic acid	-7.51	-7.39	-7.06	-6.67	-6.5
12.	P-coumaroyl hexose	-7.40	-6.39	-6.23	-6.18	-5.75
13.	Quinic acid	-7.55	-7.51	-6.8	-6.07	-5.69
14.	Rivastigmine	-6.67	-6.33	-6.47	-6.23	-5.99

Intermolecular energy is directly proportional to binding energy. We found a decrease in intermolecular energy of all the phytoconstituents with a simultaneous decrease in the binding energy. The phytoconstituents showed intermolecular energy ranging between − 8.17 kcal/mol to -5.54 kcal/mol (Table 5). 4-hydroxy coumarin had better intermolecular energy (-8.17 kcal/mol) when compared to the standard (-6.67 kcal/mol). This result further proved that 4-hydroxy coumarin and Ferulic acid consist of better anti-cholinesterase activity compared to the standard rivastigmine.

The amino acid residues responsible for the docking of 4- Hydroxy Coumarin against Adenosine A2A receptor was found to be PHE A : 255, CYS A : 259, CYS A : 262, ALA A : 265 (Fig. 3). The amino acid residues responsible for the docking of Ferulic Acid against acetylcholinesterase receptor was found to be ARG A : 293, ARG A : 296, ARG A : 304 (Fig. 4). The standard rivastigmine against acetylcholinesterase receptor was found to be ASP A : 1002, ALA A: 1043, THR A :1004 (Fig. 5).

IR spectral Interpration of 4-hydroxy coumarin

The infrared (IR) spectrum of 4-hydroxycoumarin is primarily defined by the presence of its hydroxy (-OH) group and the lactone carbonyl moiety. The structure typically exists as a coumarin-type system rather than its chromone tautomer in the solid state. The spectra of 4-hydroxycoumarin resemble the OH-vibrations in carboxylic acids in the solid state due to intense hydrogen bonding, with appearing near 3000 cm^{-1} and near 1310 cm^{-1} (Fig. 6). Carbonyl Shift is present at the 3-position, the frequency can found in 1670 cm^{-1} due to changes in hydrogen bonding strength. Hence, from the spectra it was found that, the compound is 4-hydroxy coumarin.

IR spectral Interpration of Ferulicacid

The IR spectrum of ferulic acid (4-hydroxy-3-methoxycinnamic acid) is characterized by functional groups typical of phenolic acids: a carboxylic acid, a phenolic hydroxy, a methoxy group, and an aromatic ring conjugated with an alkene. A strong, broad band characteristic of the hydroxy group in phenolic compounds was found in 3434 cm^{-1} with a shoulder at 3320 cm^{-1} indicating multiple interaction centers or complex hydrogen bonding networks between molecules in Ferulic acid (Fig. 7). Characteristic OH-stretching vibrations for carboxylic acid dimers may grow at 2600 cm^{-1} and 2700 cm^{-1} in specific environments, such as when ferulic acid is adsorbed on surfaces. Hence the spectrum was found that, the compound is Ferulic acid.

Mass spectral Interpration of 4-hydroxy coumarin

The mass spectrum of 4-hydroxycoumarin is characterized by a strong molecular ion and a very distinct fragmentation pattern that reflects its stable bicyclic structure and keto-enol tautomerism. In the spectrum the parent ion, representing the molecular weight of 4-hydroxycoumarin was observed at 163 m/z (Fig. 8). The peak at m/z 121 is a critical diagnostic tool; its high intensity is a clear indicator of the specific structural fragmentation unique to the 4-hydroxycoumarin nucleus.

Mass spectral Interpration of Ferulic acid

The mass spectral interpretation of Ferulic acid varies depending on the ionization technique used. Base peak representing the intact molecule which was observed in 194 m/z. Cleavage from the methoxy group was observed in 179 m/z. (Fig. 9). The obtained mass spectral interpratation was found as Ferulic acid.

IN VITRO ACHE INHIBITORY ACTIVITY OF THE PHYTOCONSTITUENTS

An increase in AChE leads to an increase in breakdown of ACh to acetate and choline, leading to the development of neurodegenerative disease. Usually AChE inhibitors are used in the treatment of neurodegenerative disease. When AChE inhibition occurs, it results in breakdown of acetylcholine into acetate and choline and it is measured spectroscopically. The absorbance of all the selected compounds 4-Hydroxy coumarin, and Ferulic acid decreased upon increasing the concentration in a dose dependent manner. The percentage inhibition was calculated for all compounds and for standard. A dose dependent increase in percentage of inhibition was observed for standard.

Table 6
In vitro AChE inhibitory activity of selected compounds

S. No.	Concentration (µg/ml)	Percentage of inhibition		
		Ferulic acid	4-Hydroxy coumarin	Rivastigmine
1	2	38.1462	33.1464	4.3014
2	4	42.5126	56.3236	11.5204
3	8	54.9121	64.8614	24.9201
4	16	66.8128	77.3614	27.2521
5	32	79.9124	81.9641	47.6213
6	64	86.3146	94.3614	54.1131

The selected compounds exhibited the highest AChE inhibitory activity than the standard rivastigmine. The inhibition constant (IC_{50}) of Ferulic acid was found to be 7.5468 ± 1.42 µg/ml and for 4- hydroxy coumarin was found to be 3.4562 ± 0.84 µg/ml when compared to the standard rivastigmine showed 3.913 ± 0.48 µg/ml (Table 6). 4- hydroxy coumarin was showed noteworthy AChE inhibitory activities when compared to the Ferulic acid and the standard.

DISCUSSION

Research indicates that the methanol extract of *Ailanthus excelsa* possesses a comprehensive range of antimicrobial capabilities, successfully inhibiting almost all evaluated bacterial strains with the notable exceptions of *Bacillus subtilis* and *Staphylococcus aureus*. Interestingly, the Gram-negative bacterium *Escherichia coli* displayed the highest vulnerability, implying that methanol may efficiently isolate polar phytochemicals that specifically target Gram-negative organisms. These distinct levels of sensitivity across different bacterial strains are likely driven by variations in cell wall composition and outer membrane permeability (Patil, 2025).

The stem bark extract of *Ailanthus excels* along with its respective fractions demonstrates potent cytotoxic, anti-inflammatory, and antioxidant properties, with the highest efficacy observed in the

chloroform fraction. Analytical techniques using GC-MS coupled with *in silico* modeling identified phenolics and caftaric acid as the primary bioactive constituents. These insights suggest that such compounds hold significant therapeutic promise for managing malignancies, inflammatory disorders, and diseases associated with oxidative stress (Sapkal et al., 2023).

Characterized as a polyphenol-dense extract, the n-butanol fraction generally exhibits distinct spectral bands during Fourier-transform infrared (FTIR) spectroscopy. The specific functional groups mapped by these absorption peaks align closely with the therapeutic properties associated with the plant. Consequently, the peak profiles generated through FTIR analysis verify the presence of these characteristic functional groups within *Ailanthus excelsa*.

Existing literature indicates that *Ailanthus excelsa* contains an array of bioactive phytoconstituents, including selinidin, trans-piceatannol, p-hydroxyphenethyl anisate, 4-O-feruloylquinic acid, p-coumaroylquinic acid, 4-hydroxycoumarin, ferulic acid, salicylic acid, 5-hydroxyferulic acid, caffeic acid, malic acid, p-coumaroyl hexose, and quinic acid. The functional configurations of these identified molecules were successfully validated via the FTIR spectra. Driven by these structural confirmations, these compounds were selected for subsequent *in silico* modeling and *in vitro* assays targeting the acetylcholinesterase enzyme to explore their therapeutic potential in mitigating neurodegenerative disorders.

Lipinski's rule of five serves as a foundational benchmark for evaluating the interplay between a molecule's physicochemical properties and its pharmacokinetic profile, particularly concerning oral absorption. Within this framework, *in silico* profiling assesses the drug-likeness of specific compounds relative to established therapeutics. Favorable oral bioavailability is typically anticipated when an agent satisfies standard structural boundaries: an octanol-water partition coefficient Log P < 5, a molecular weight MW < 500Da, no more than 10 hydrogen bond acceptors (HBA), and fewer than 5 hydrogen bond donors (HBD). Additionally, structural flexibility is quantified via the number of rotatable bonds, which should remain below 10. Aqueous solubility remains another critical metric, as it directly dictates systemic drug absorption kinetics (Sicak, 2021). In this investigation, all thirteen isolated phytoconstituents strictly conformed to Lipinski's parameters. Consequently, the entire set of molecules was advanced to *in silico* molecular docking simulations targeting the acetylcholinesterase (AChE) enzyme.

This approach mirrors previous drug design strategies; for instance, Hamulakova et al. (2017) designed a novel series of acridine-coumarin hybrids to assess their inhibitory efficacy against both AChE and butyrylcholinesterase (BuChE). Their newly synthesized analogues, specifically compounds 9a–d, demonstrated superior potency against human AChE compared to the reference drug 7-MEOTA. Among these, derivative 9b emerged as the most potent inhibitor, yielding an IC_{50} value of 5.85 15 μM, which marks a significant improvement over the 15 μM baseline of 7-MEOTA. Computational modeling was subsequently utilized to map the specific binding configurations of configurations 9b, 9c, and 9f within the active sites of human AChE and BuChE.

Computational screening using AutoDock 4.2 software was executed to evaluate the competitive ACE inhibitory capabilities of a specific alkaloids, including ajmaline, atropine, caffeine, and emetine. The molecular docking assays revealed that all evaluated alkaloids demonstrated robust binding affinities, with binding energies spanning – 9.75 kcal/mol to -4.98 kcal/mol, standing in favorable comparison to the reference standard's score of (-5.38 kcal/mol). This strong affinity profile was further supported by corresponding inhibition constants ranging between (77.38 nM to 225.41 μM), alongside intermolecular energy values measured from (-11.84 kcal/mol to -6.17 kcal/mol) (Madeswaran and Asokkumar, 2015).

In a separate investigation into cholinesterase inhibition, Park et al. (2017) scrutinized a novel series of 3,4-dihydroquinazoline derivatives to map their inhibitory profiles against both AChE and BuChE. Within this structural library, compounds 8b and 8d emerged as the most potent agents against BuChE, delivering 45nM and 62nM, respectively. These figures translate to an impressive 146-fold and 161-fold higher selectivity for BuChE over AChE. To clarify the underlying atomic mechanisms driving this selectivity, the authors applied molecular docking simulations. The computational models confirmed that analogues 8b and 8d concurrently occupy the catalytic anionic site (CAS) and the peripheral site (PS) of BuChE, generating significantly stronger interaction energies than those seen with AChE. Enzyme kinetics further validated this dual-site engagement, showing non-competitive/mixed-type inhibition profiles for both lead configurations.

In the current study, found a decrease in binding energy of all the phytoconstituents against acetylcholinesterase target enzyme. The phytoconstituents showed binding energy ranging between – 8.36 kcal/mol to -3.82 kcal/mol. 4-hydroxy coumarin had excellent binding energy (-8.36 kcal/mol) when compared to the standard (-5.21 kcal/mol). This result further proved that 4-hydroxy coumarin and Ferulic acid consist of notable anti-cholinesterase activity compared to the all other phytoconstituents and standard rivastigmine.

The phytoconstituents showed inhibition constant ranging between 4.67 μM to 44.91 mM. 4-hydroxy coumarin had excellent binding energy 4.67 μM when compared to the standard 22.62 μM. This result further proved that 4-hydroxy coumarin and Ferulic acid consist of notable cholinesterase inhibition constant values compared to the all other phytoconstituents and standard rivastigmine.

Intermolecular energy is directly proportional to binding energy. We found a decrease in intermolecular energy of all the phytoconstituents with a simultaneous decrease in the binding energy. The phytoconstituents showed intermolecular energy ranging between – 8.17 kcal/mol to -5.54 kcal/mol. 4-hydroxy coumarin had better intermolecular energy (-8.17 kcal/mol)when compared to the standard (-6.67 kcal/mol). This result further proved that 4-hydroxy coumarin and Ferulic acid consist of better anti-cholinesterase activity compared to the standard rivastigmine.

The amino acid residues responsible for the docking of 4-o-feruloylquinic acid against AChE acetylcholinesterase was found to be PHE A : 168, ILE A : 274, ASN A : 253, LEU A : 249, VAL A : 84, ALA A : 63, ILE A : 66 (Fig. 19) and 4- Hydroxy Coumarin against Adenosine A2A receptor was found to be PHE A : 255, CYS A : 259, CYS A : 262, ALA A : 265. The amino acid residues responsible for the docking

of Ferulic Acid against acetylcholinesterase receptor was found to be ARG A : 293, ARG A : 296, ARG A : 304 and p-coumaroyl hexose against acetylcholinesterase receptor was found to be HIS A : 230, ARG A : 291, ARG A : 293, ARG A : 296.

The amino acid residues responsible for the docking of 5-Hydroxy Ferulic Acid against acetylcholinesterase receptor was found to be LYS A : 122, VAL A : 46, TRP A : 32, CYS A : 28 and rivastigmine against acetylcholinesterase receptor was found to be ASP A : 1002, ALA A: 1043, THR A :1004.

By coordinating isolated flavonoid extracts, four distinct coordination metal complexes were successfully engineered and validated using established analytical characterization techniques. These synthesized complexes demonstrated specific colorimetric profiles, low pH characteristics, and distinct electrolytic conductivity values. Powder X-ray diffraction (XRD) metrics revealed varying degrees of structural crystallinity when comparing the raw flavonoid extracts against their corresponding metallic complexes. Additionally, Fourier-transform infrared (FTIR) spectrophotometry recorded diagnostic shifts in stretching vibrations, directly confirming the successful coordination between the metal centers and the flavonoid ligands. In electronic spectroscopy, the raw flavonoid extracts displayed primary UV-Visible absorption bands at 280 nm and 340 nm. Upon metal chelation, these bands underwent predictable bathochromic or hypsochromic shifts, giving rise to novel spectral profiles featuring three distinct peaks distributed within the 260–660 nm window. Furthermore, 1H NMR profiling demonstrated that the proton signals of the coordinated complexes shifted upfield relative to the free ligands; this shielding effect is likely driven by enhanced spin-spin coupling and improved structural planarity across the conjugated flavonoid skeleton following metal complexation (Mohsen et al., 2024).

In a separate synthetic pathway, an array of alkyl and ester derivatives was derived from the core flavonoid scaffold 3-hydroxy-2-[4-(dimethylamino)phenyl]benzopyran-4-one. This parent molecule was systematically reacted with a diverse suite of chemical reagents—specifically methyl iodide, allyl bromide, benzyl chloride, bromoacetylcoumarin, chloroacetamide, chloroacetyl chloride, phthalic anhydride, maleic anhydride, phthalimide, and cinnamoyl chloride. These substitution and condensation reactions were carried out in the presence of a potassium carbonate base, employing either acetone or dimethylformamide (DMF) as the reaction solvent matrix. The structural and physical properties of these newly synthesized molecular entities were systematically characterized using a combination of spectroscopic assays, including FTIR, 13C-NMR, and 1H-NMR. Finally, the chemical purity and reaction completion of all synthesized derivatives were verified via thin-layer chromatography (TLC) (Khdera et al., 2022).

From the physical data available from the current study,4-hydroxy coumarin and ferulic acid were established through IR, and mass spectral characterization of compounds revealed the successful confirmation of the product and further selected for the *in vitro* acetylcholinesterase inhibitory activity using Ellman’s methods.

Investigation by Vivitri et al. (2018) highlighted the growing importance of acetylcholinesterase-inhibitory peptides, which actively suppress acetylcholinesterase (AChE) activity to elevate acetylcholine concentration within cholinergic synapses, thereby reinforcing cholinergic signaling. Consequently, naturally derived peptides have emerged as a focal point of interest for isolating novel AChE inhibitors. Due to their targeted neuroprotective and therapeutic activities, these biopolymers offer substantial pharmaceutical potential for addressing neurodegenerative pathologies. Indeed, a selection of natural peptides and their engineered analogues already possess considerable commercial value and have successfully transitioned into the clinical market, with numerous others undergoing preclinical evaluations and clinical trials for varied disease states. This review centers on recent breakthroughs in natural peptide discovery and outlines their prospective application in treating cognitive decline.

Concurrently, Ghafary et al. (2018) evaluated a novel library of synthesized cinnamic acid–tryptamine hybrids developed to serve as cholinesterase inhibitors. The bioassays revealed that these synthetic derivatives displayed preferential selectivity toward butyrylcholinesterase (BChE) inhibition, while demonstrating only marginal potency against acetylcholinesterase (AChE). Among the tested library, the specific cinnamic acid–tryptamine analogue compound 7d emerged as the most potent BChE inhibitor, yielding an IC_{50} of 0.55 ± 0.04 μM.

The selected compounds exhibited the highest AChE inhibitory activity than the standard rivastigmine. The inhibition constant (IC_{50}) of Ferulic acid was found to be 7.5468 ± 1.42 mg/mll and for 4- hydroxy coumarin was found to be 3.4562 ± 0.84 mg/ml when compared to the standard rivastigmine showed 3.913 ± 0.48 mg/ml. 4- hydroxy coumarin and Ferulic acid were showed AChE inhibitory activities at a concentration below 100 μg/ml (Table 6). Further *in vivo* preclinical studies need to perform for the Ferulic acid and 4-hydroxy coumarin to develop potential drug in the management of neurodegenerative diseases.

CONCLUSION

Ailanthus excelsa Roxb. belongs to the family Simaroubaceae, which is highly diverse and studied for a wide range of potential therapeutic properties, including antioxidant, anti-inflammatory, antimicrobial, and Antischistosomal activities. In the current study, the characterization from the FTIR found the 13 active phytoconstituents and which further predicted for drug likeness assessments. The selected phytoconstituents were screened for *in silico* molecular modelling studies against acetylcholinesterase inhibition. Based on the docking score and orientations, 4-hydroxy coumarin and Ferulic acid exhibited an excellent inhibitory potential for acetylcholinesterase target inhibition compared to the standard Rivastigmine. The *in vitro* acetylcholinesterase inhibitory assay was performed for the 4-hydroxy coumarin and Ferulic acid using Ellman's method. From the *in vitro* enzyme inhibition assay, 4-hydroxy coumarin and Ferulic acid were found to possess noteworthy inhibition against AChE. It can be concluded that, 4-hydroxy coumarin and Ferulic acid has possess potential role in the neuroprotection and it could be further develop as a potential drug candidate against neurodegenerative diseases.

Further preclinical and clinical studies needs to perform on the 4-hydroxy coumarin and Ferulic acid to prove its role in the management of neurodegenerative diseases.

Declarations

CONFLICT OF INTEREST

The authors declare that there are no conflicts of interest for this work.

Author Contribution

V.M. and M.K. wrote the main manuscript text and M.K. carried out the work and prepared figures. All authors reviewed the manuscript.

References

1. Aaron DG, Paraminder D, James S (2017) Neurodegenerative disease: models, mechanisms, and a new hope. Dis Models Mech 10(5):499–502
2. Ajit K, Parul K, Kritika G, Karan A (2018) Pathophysiology and Management of Alzheimer's Disease: An Overview. Anal Pharm Res 9(2):226–323
3. Babitha PP, Sahila, Bandaru S, Nayarisseri A, Sureshkumar S (2015) Molecular Docking and pharmacological investigations of rivastigmine-fluoxetine and coumarin–tacrine hybrids against acetyl choline esterase. Bioinformation 11(8):378–386
4. Bang D, Kim J, Song H, Kim S (2025) ADME-drug-likeness: enriching molecular foundation models via pharmacokinetics-guided multi-task learning for drug-likeness prediction. Bioinformatics 41(1):i352–i361
5. Crampon K, Giorkallos A, Deldossi M, Baud S, Steffenel LA (2022) Machine-learning methods for ligand-protein molecular docking. Drug Discovery Today 27(1):151–164
6. Das B, Baidya ATK, Mathew AT, Yadav AK, Kumar R (2022) Structural modification aimed for improving solubility of lead compounds in early phase drug discovery. Bioorg Med Chem 56:116614
7. Ellman GL, Courtney DK, Andres V, Featherstone RM (1961) A new and rapid colorimetric determination of acetylcholinesterase activity. Biochem Pharmacol 7:88–95
8. Ghafary S, Najafi Z, Mohammadi-Khanaposhtani M, Nadri H, Edraki N, Ayashi N, Larijani B, Amini M, Mahdavi M (2018) Novel cinnamic acid-tryptamine hybrids as potent butyrylcholinesterase inhibitors: Synthesis, biological evaluation, and docking study. Archiv der Pharmazie (Weinheim) 351(10):e1800115
9. Hamulakova S, Janovec L, Soukup O, Jun D, Kuca K (2017) Synthesis, in vitro acetylcholinesterase inhibitory activity and molecular docking of new acridine-coumarin hybrids. Int J Biol Macromol 10(A):333–338

10. Karami TK, Hailu S, Feng S, Graham R, Gukasyan HH (2022) Eyes on Lipinski's rule of five: A new Rule of Thumb for physicochemical design space of ophthalmic drugs. J Ocul Pharmacol Ther 38(1):43–55
11. Khdera HA, Saad SY, Moustapha A, Kandil F (2022) Synthesis of new flavonoid derivatives based on 3-hydroxy-4'-dimethylamino flavone and study the activity of some of them as antifungal. Heliyon, 8(12), e12062
12. Madeswaran A, Asokkumar K (2015) Evaluation of inhibitory affinity potential of the alkaloids against crystal structure of human angiotensin-converting enzyme using Lamarckian genetic algorithm. Adv Traditional Med 15:183–189
13. Madeswaran A, Brahmasundari S, Mohan S, Parasuraman P (2024) *In silico* evaluation of some commercially available terpenoids as spike glycoprotein of SARS-CoV-2 – inhibitors using molecular dynamic approach. *Journal of Biomolecular Structure and Dynamics*, *42*, 1072–1078
14. Madeswaran A, Mohan S (2023) Neuroprotective effects of terpenoids against streptozotocin-nicotinamide-induced diabetic rats: An in silico, in vitro and in vivo study. Int J Biol Macromol 247:125817–125822
15. Mohsen EMA, Saeed AAM, Yahia AAB (2024) Synthesis, characterization, and bioactivity evaluation of several divalent transition metal ion-bioflavonoid complexes. Results Chem 7:101535
16. Natesh S, Philippe V, Shivalika T, Jean-Luc P, Katya T, Bruno VO (2023) Drug discovery and development: introduction to the general public and patient groups. Front Drug Discovery 3:1–5
17. Park B, Nam JH, Kim JH, Kim HJ, Onnis V, Balboni G, Lee K, Park JH, Catto M, Carotti A, Lee JY (2017) 3,4-Dihydroquinazoline derivatives inhibit the activities of cholinesterase enzymes. Bioorg Med Chem Lett 27(5):1179–1185
18. Patil MS (2025) Phytochemical, Spectral Analysis and Antimicrobial Evaluation of Leaf Extracts from *Ailanthus excelsa* Roxb. J East-West Thought 15(2):801–808
19. Prafulla S, Lata P, Nusrat S, Priya R (2021) Design, synthesis and pharmacological screening of novel flavone derivatives. Syst Reviews Pharm 12(12):3817–3821
20. Prasasty V, Radifar M, Istyastono E (2018) Natural peptides in drug discovery targeting Acetylcholinesterase. Molecules 23(9):2344
21. Rashed K, Said A, Ahmed M (2013) Antiviral activity and phytochemical analysis of Ailanthus excelsa Roxb bark. J For Prod Industries 2(3):30–33
22. Sacan O, Yanardag R (2010) Antioxidant and antiacetylcholinesterase activities of chard (*Beta vulgaris* L. Var. *Cicla*). *Food and Chemical Toxicology*, *48*, 1275–1280
23. Sapkal PR, Tatiya AU, Firke SD, Redasani VK, Gurav SS, Ayyanar M et al (2023) Phytochemical profile, antioxidant, cytotoxic and anti-inflammatory activities of stem bark extract and fractions of *Ailanthus excelsa* Roxb.: in vitro, in vivo and in silico approaches. Heliyon 9(5):e15952–e15960
24. Sasidharan S, Chen Y, Saravanan D, Sundram KM, Yoga Latha L (2011) Extraction, isolation and characterization of bioactive compounds from plants' extracts. Afr J Tradit Complement Altern Med 8(1):1–10

25. Shin CY, Kim HS, Cha KH et al (2018) The Effects of Donepezil, an Acetylcholinesterase Inhibitor, on Impaired Learning and Memory in Rodents. Biomolecules Ther (Seoul) 26(3):274–281
26. Sicak Y (2021) Synthesis, predictions of drug-likeness, and pharmacokinetic properties of some chiral thioureas as potent enzyme inhibition agents. Turk J Chem 46(3):665–676
27. Tang L, Zhang S, Yang J, Gao W, Cui J, Zhuang T (2004) A Novel approach to the synthesis of 6-Amino-7-hydroxy-flavone. Molecules 9:842–848
28. Tokali FS, Demir Y, Turkes C, Dincer B, Beydemir S (2023) Novel acetic acid derivatives containing quinazolin-4(3H)-one ring: Synthesis, in vitro, and in silico evaluation of potent aldose reductase inhibitors. Drug Dev Res 84(2):275–295
29. Vargas-Madriz AF, Kuri-García A, Vargas-Madriz H, Chavez-Servín JL, Ferriz-Martinez AR, Hernandez-Sandoval LG, Guzman-Maldonado SH (2020) Phenolic profile and antioxidant capacity of Pithecellobium dulce (Roxb) Benth: a review. J Food Sci Technol 57(12):4316–4336
30. Vijayabaskaran M, Ishfaq S, Madeswaran A (2025) In silico molecular docking analysis of some commercially available tannins and evaluation of in vitro acetylcholinesterase inhibitory activity of ellagic acid for the management of Alzheimer's disease. J Technol 13(1):742–752
31. Wadood A, Ahmed N, Shah L, Ahmad A, Hassan H, Shams S (2013) In-silico drug design: An approach which revolutionarised the drug discovery process. OA Drug Des Delivery 1(1):3–8

Figures



Figure 1

Refined structure of acetylcholinesterase enzyme from RCSB-PDB (1GQR)

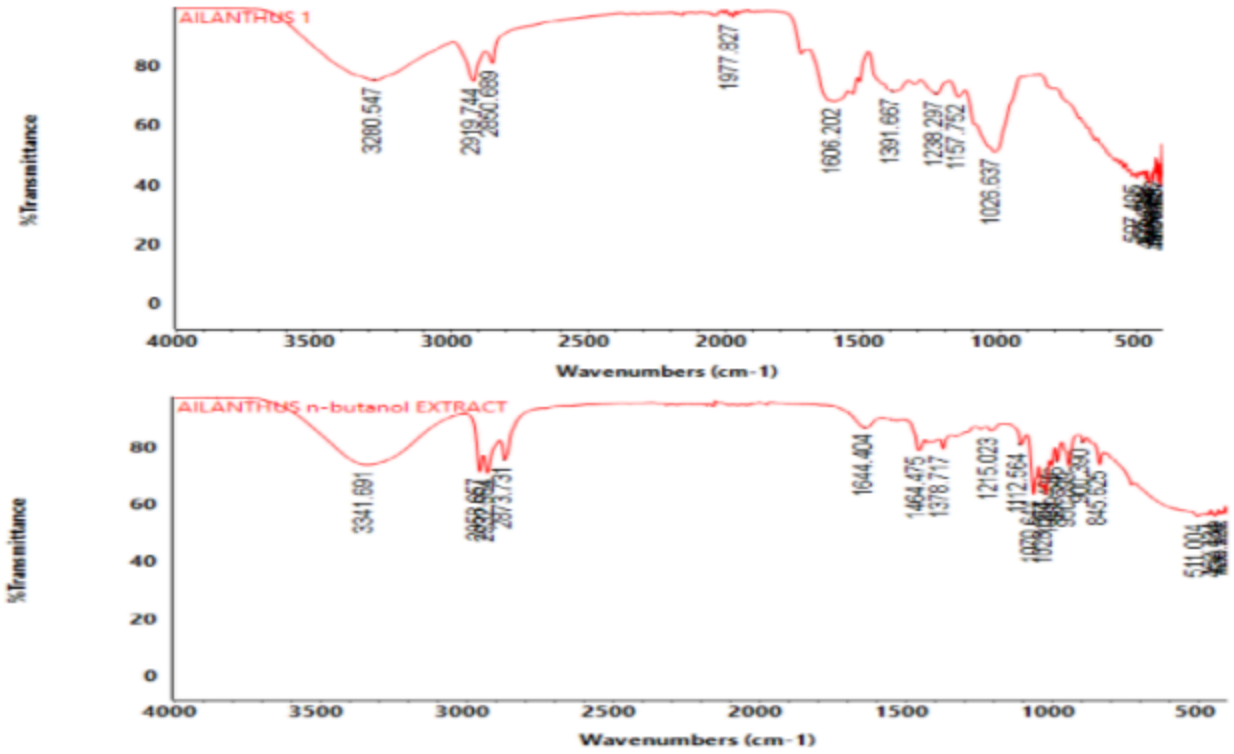


Figure 2

FTIR of Dry powder and n-butanol extract of *Ailanthus excels*

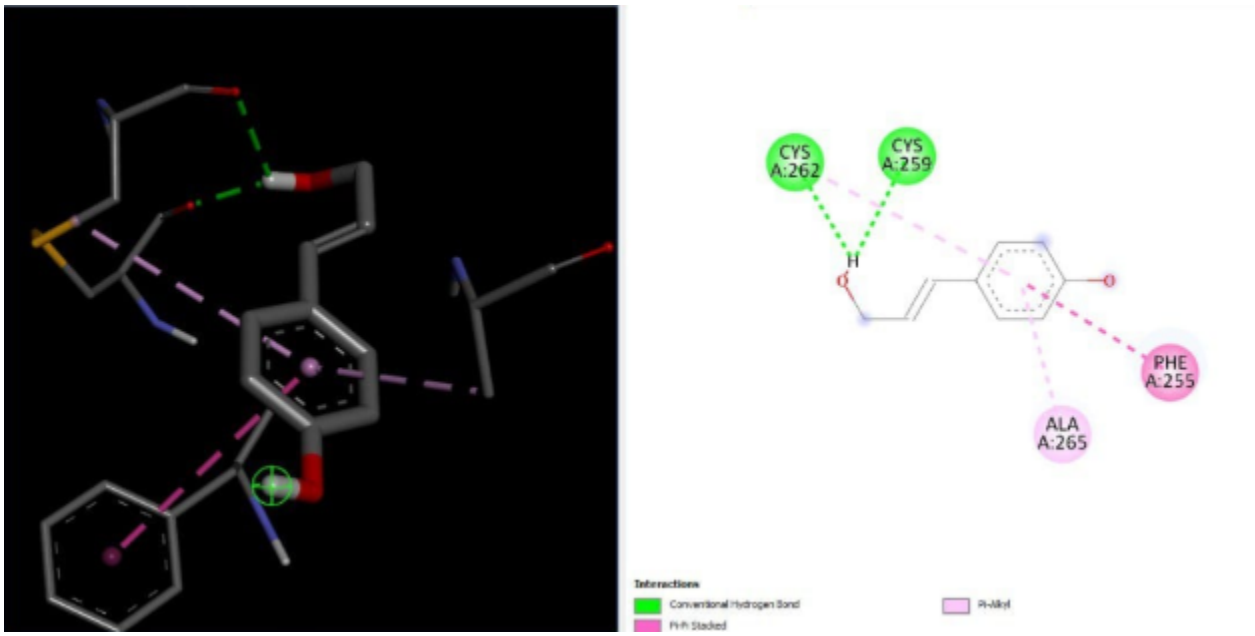


Figure 3

Binding orientation of 4-hydroxy coumarin against acetylcholinesterase target enzyme

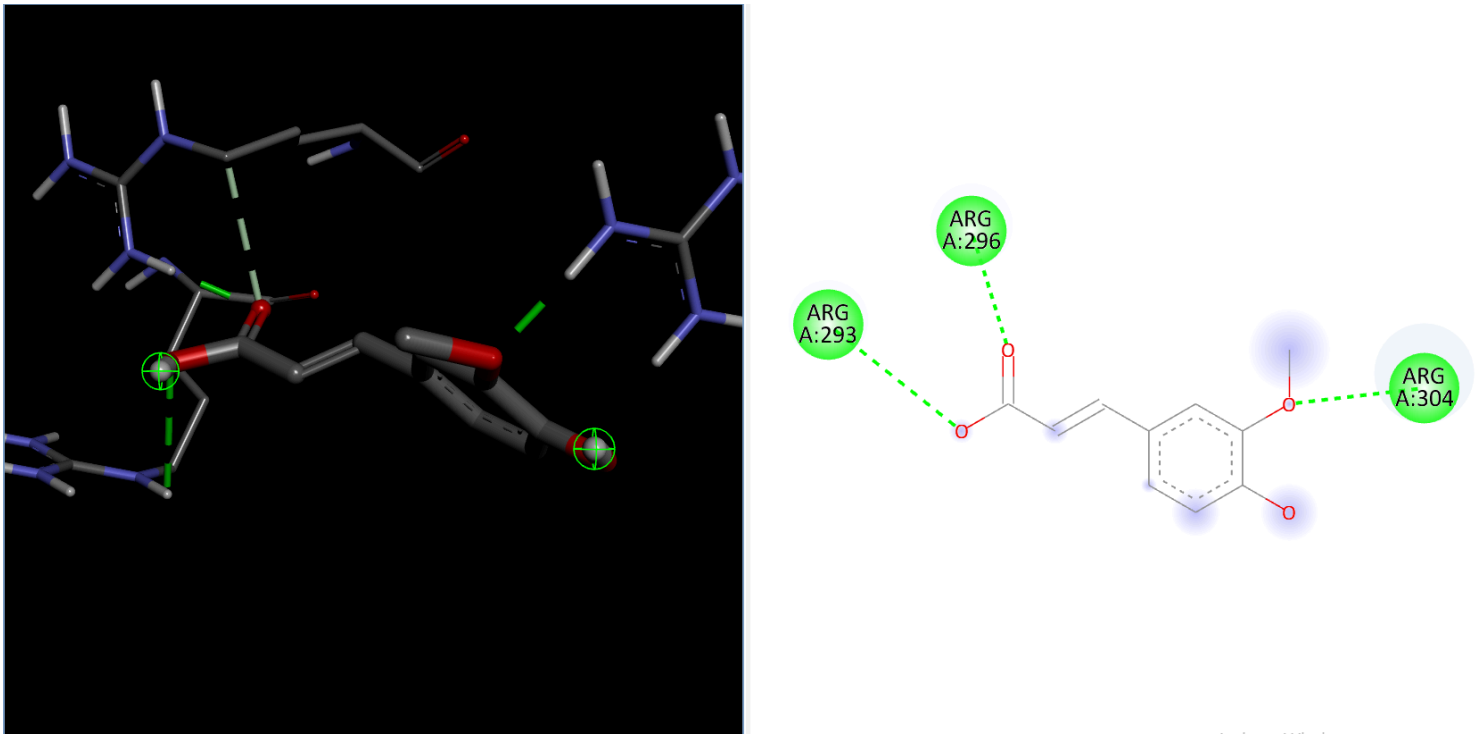


Figure 4

Binding orientation of ferulic acid against acetylcholinesterase target enzyme

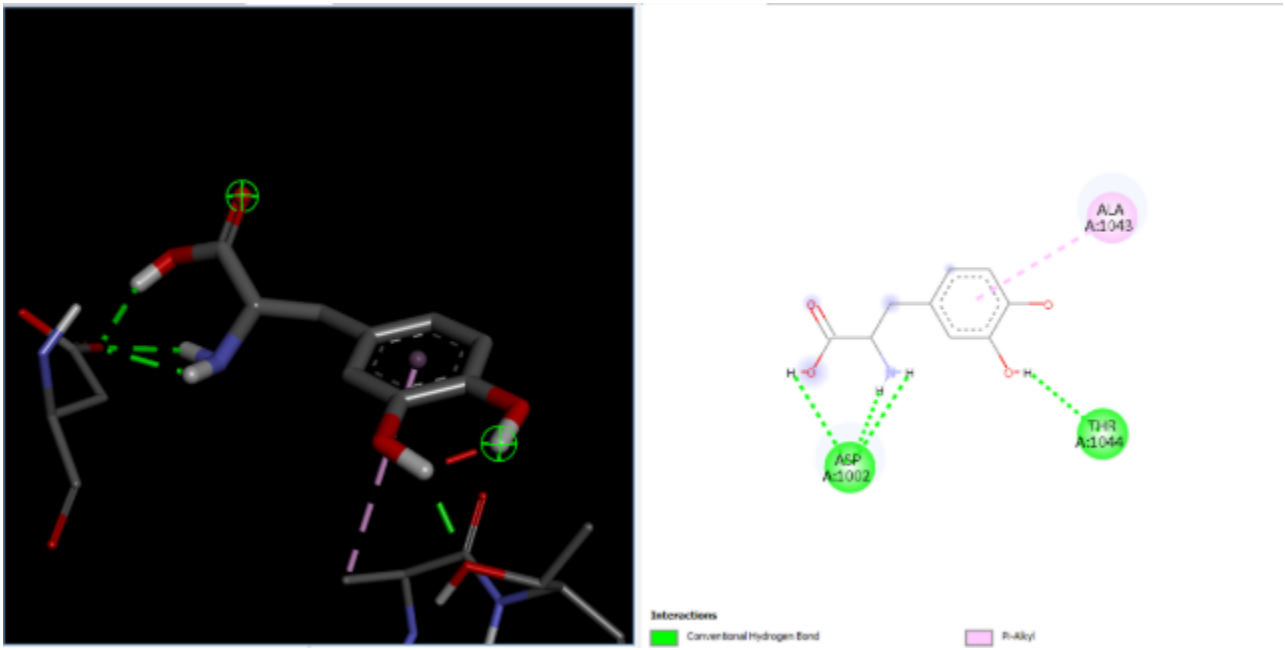


Figure 5

Binding orientation of standard drug [rivastigmine] against acetylcholinesterase target enzyme

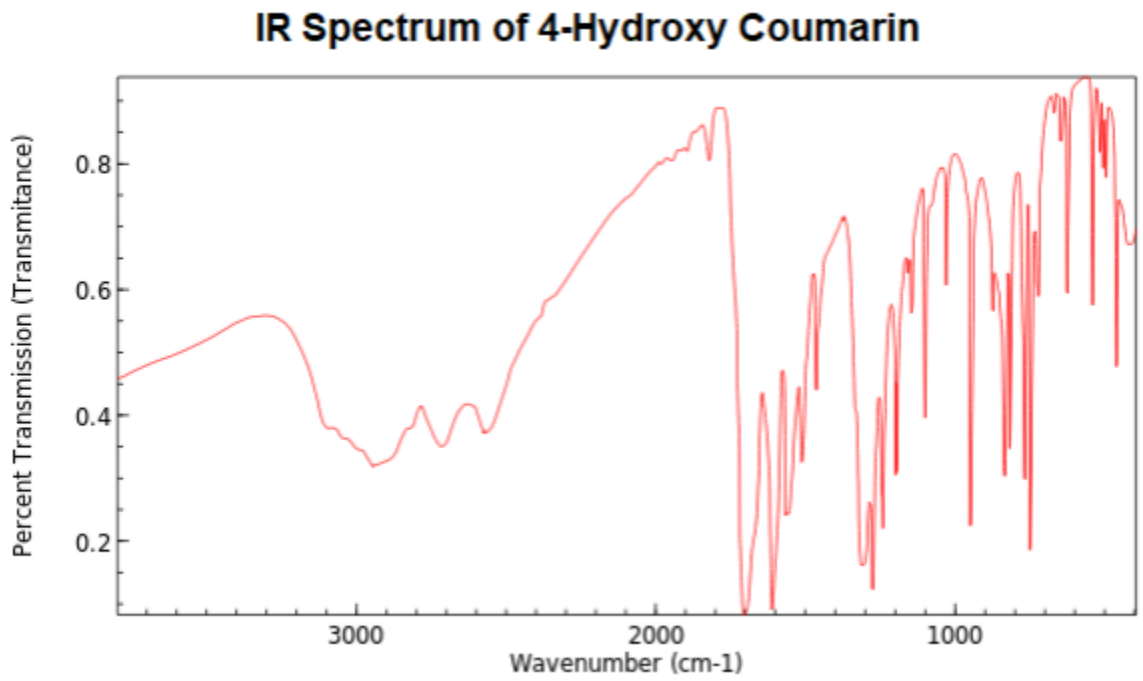


Figure 6

IR spectral Interpration of 4-hydroxy coumarin

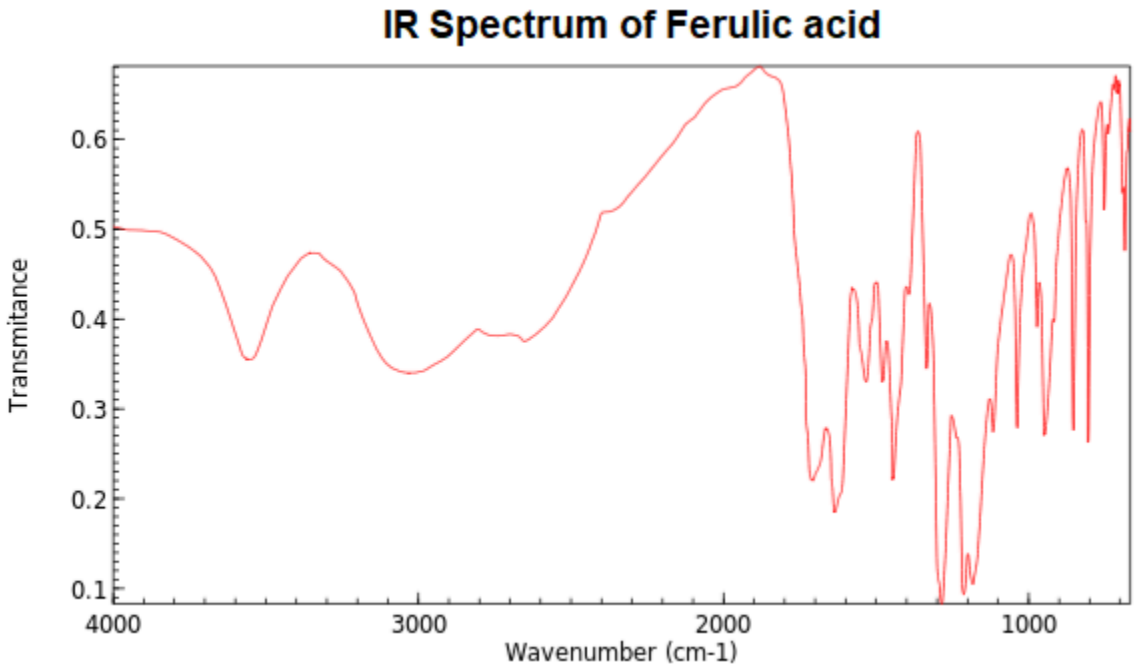


Figure 7

IR spectral Interpration of Ferulic acid

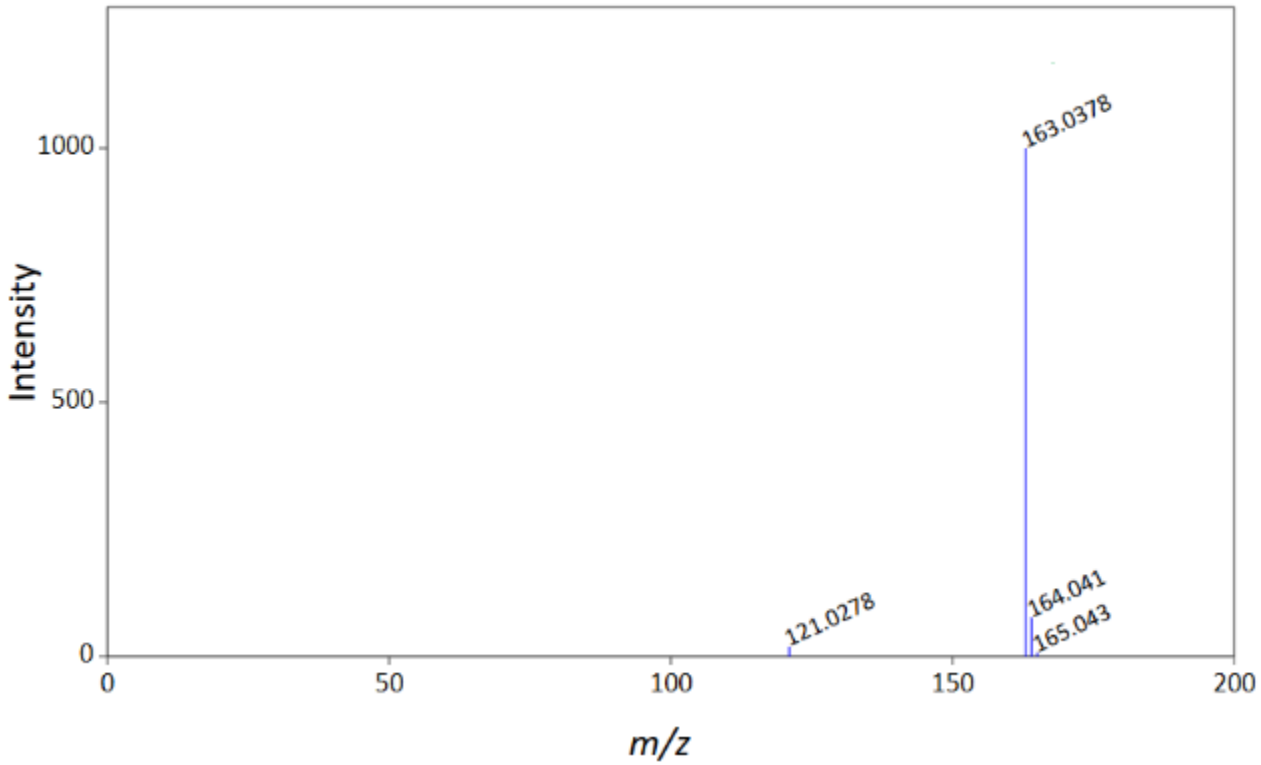


Figure 8

Mass spectral Interpration of 4-hydroxy coumarin

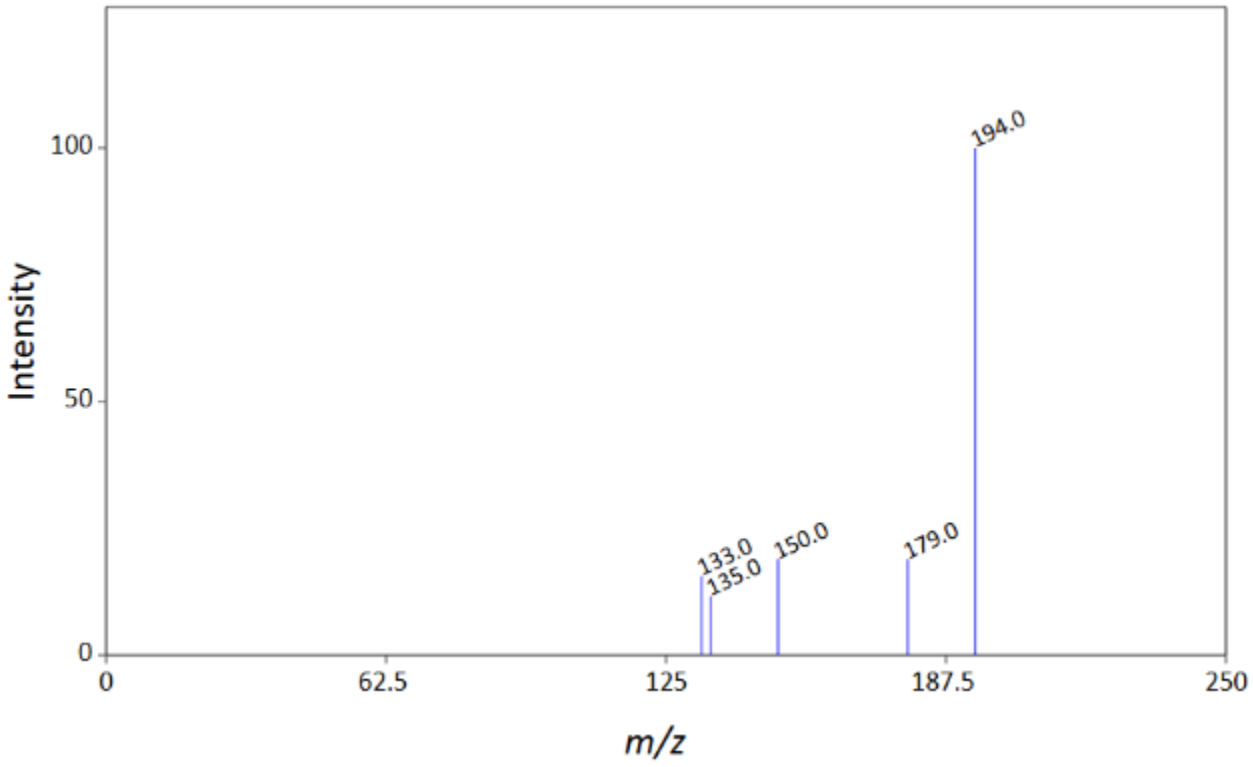


Figure 9

Mass spectral Interpration of Ferulic acid